INFRARED SIGNATURE ASSESSMENT OF AN AGILE, HIGHLY SWEPT FLYING WING CONFIGURATION

E. Lindermeir
DLR – Remote Sensing Technology Institute
P.O. Box 1116, Weßling, D-82230, Germany

M. Rütten
DLR – Institute of Aerodynamics and Flow Technology
Busenstraße 10, Göttingen, D-37073, Germany

Abstract

DLR´s capabilities in aircraft design are spread over many institutes which are located at various sites in Germany. With the *Mephisto* project DLR aims at combining this distributed expertise. The paper at hand reports on one aspect of this effort, the reduction of the infrared (IR) signature of a wing only configuration´s propulsion system. This was achieved through the collaboration of three DLR institutes, namely the Institute of Propulsion Technology (Cologne), Institute of Aerodynamics and Flow Technology (Göttingen), and the Remote Sensing Technology Institute (Oberpfaffenhofen). The work on engine design performed at the Institute of Propulsion Technology is described in a separate paper. Thus, the focus here is on the achievements in infrared modeling and the aerodynamic design, especially of the exhaust system. The paper presents the capabilities of MIRA (Model for Infrared Signature Analysis). This tool had certain capabilities added and then was applied in Mephisto to predict the IR signature of different variants of the configuration´s exhaust duct. The result of this design effort is a large reduction of the IR emission caused by the exhaust gases. However, the simulations show that low observability is not yet achieved.

Keywords

Aeronautics, Aircraft, Infrared Signature, MIRA, TAU

1. INTRODUCTION

A major design goal in the development of military air vehicles is low observability. Thus, radar-, electro-optic (EO) and acoustic signatures must be kept as low as possible. Unfortunately this demand causes severe design constraints which have negative effects on aircraft operation. A low radar cross section, for example, may be achieved by omitting the vertical tail of an aircraft. However, this decision greatly reduces yaw stability. Similarly, the IR signature of the exhaust gases may be lowered by installation of a low power engine. But obviously this will lead to reduced agility. Therefore, the design process of a military aircraft, as most engineering tasks, consists of searching for acceptable compromises and finding alternative solutions which may replace well-known methods that negatively impact signatures (e.g. using thrust vector control to achieve yaw stabilization, or mixing and/or active cooling to reduce exhaust gas temperature).

The design task becomes easier, if reliable prediction tools are available. They help to quantify the consequences of design decisions as early as possible. As military aircraft design comprises many different technologies, such as aerodynamics, jet engines, structural- and flight mechanics, flight control systems, signatures, etc., it is necessary to couple the tools of different experts. The demonstration of such multidisciplinary, coupled, virtual design process is the central task of DLR´s Mephisto project. The configuration which results from in-house collaboration but also from close contacts to industry is a generic unmanned combat air vehicle (UCAV) called MULDICON (see Fig. 1).

doi:10.25967/480004

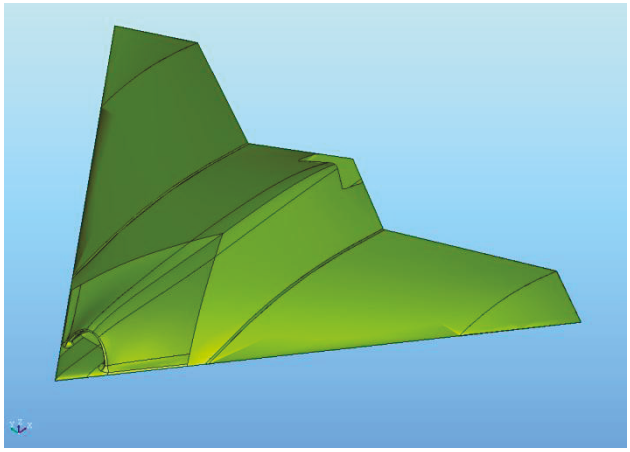

Fig. 1 The generic "MULDICON" UCAV

With regard to IR signatures DLR´s Remote Sensing Technology Institute has developed a model which permits predictions of IR signatures of air vehicles in their natural environment. This MIRA tool [1, 2] is introduced in section 2.

The IR tool can determine the radiance of exhaust gases only, if the distributions of temperature, pressure and species concentrations in the aircraft´s plume are known. These are determined at the Institute of Aerodynamics and Flow Technology using their TAU code [3], a well-established computational fluid dynamics (CFD) solver. This work and the design of the various variants of the exhaust duct are the topic of sections 3 and 4.

Finally, Section 5 presents comparisons of the IR signatures resulting for the various designs.

2. IR-SIGNATURE MODEL MIRA

Surface radiance

The radiance emitted from surfaces is determined by the surface temperature, its emissivity, its reflectivity and the surface environment.

The surface temperatures in flight conditions are usually above ambient temperature, as there are various heat sources inside the aircraft (engine, exhaust gas/duct, avionic). Moreover, at transonic flight velocities aerothermal heating causes an additional temperature rise.

The emissivity depends not only on the material/coating but is also a function of wavelength and the direction in which the radiation is emitted. Similarly, the reflectivity depends on wavelength as well as incident, and reflected directions. To permit a general treatment material properties in MIRA are described by Bidirectional Reflectance Distribution Functions (BRDF). Based on these MIRA infers directional emissivities. This ensures consistency of emissive and reflective properties. Spectrally resolved calculations are necessary anyway, as the radiance emitted by exhaust gases and also the influence of the atmosphere exhibits a strong spectral dependence.

Altogether, MIRA calculates the radiance of surface emitted into a certain direction as the sum of the surface emission due to temperature and emissivity and the reflected radiance due to radiation incident onto the surface from the environment (half-space) over the surface.

Cavity radiance (inlet, exhaust duct)

Realistic modeling of cavity radiance is required to model the influence of the inlet and the exhaust duct. In MIRA this capability is achieved by a ray-tracer in connection with Monte Carlo integration. Two methods were implemented to treat multiple reflections. Both are variants of path-tracing and are described in [4]. The simpler procedure constructs paths, i.e. sequences of rays, from the camera only. The more sophisticated but also computationally more expensive technique forms a path from two subpaths. The first sub-path is generated starting from the camera, as in the simpler method. The second sub-path starts from a randomly selected surface facet. These paths are then connected to form one path along which the radiance arriving at the camera is determined. The probability density function to select a surface facet for the generation of the second sub-path is proportional to the emitted radiance of the surface. In this manner, more emissive facets are chosen with higher probability. As a consequence, the effectiveness of path-tracing is greatly improved, as surfaces with large radiance contributions to the camera image are found with high probability, i.e. the Monte Carlo integration converges more quickly. In addition, hot parts which are difficult to find, if paths start from the camera only, are much easier taken into account.

Exhaust gas radiance

The modeling of the spectral radiance emitted by hot gases is a decisive component of an IR signature model for aircraft and rockets. These predictions are not only needed to describe the

influence of the plume after the exhaust gases are release to the atmosphere. Emission and absorption of the gases in the cavities, especially the hot gases in the exhaust duct, must not be neglected. Their influence must be taken into account by the multiple reflection models which treat cavity radiance.

To model radiance propagation in hot gases, the state variables pressure, temperature and species concentrations of the gas are needed. These are determined by a CFD calculation (see section 3). A further input is a spectroscopic database, which provides data to compute the absorption cross sections of the various species in the exhaust. For aircraft plumes, mainly the IR-active gases H_2O, CO_2, and CO are of interest.

With the spectroscopic database HITEMP 2010 [5] available it is in principle possible to perform the required calculations at extremely high spectral resolution. However, considering that most relevant threats employ broad band sensors, the vastly increased effort of high resolution (line-by-line) calculations is not warranted. Therefore MIRA uses a band model [6] which features a spectral resolution of 5 cm^{-1} and provides results with orders of magnitude lower computational effort. The band model database has been updated based on HITEMP 2010 at the Remote Sensing Technology Institute [7].

Atmosphere and ground radiance

Radiance propagation in the atmosphere is a further topic to be modeled. The atmospheric influence relates mainly to the absorption between aircraft and observer. However, the radiance of the sky must also be determined, as it represents the background in scenarios in which the observer is on the ground or at a lower altitude than the aircraft. Moreover, in such situations the radiation emitted by the ground is also of great importance. Ground IR emission may actually exceed the emission of the airplane´s surfaces, as the ground is often warmer than the aircraft at altitude. Ground radiation is reflected at the lower aircraft surface and may reach the observer. This effect may create a large contrast of the aircraft signature against the low IR radiance of the sky.

MIRA is coupled to the atmospheric model MODTRAN [8, 9] to account for the influence of atmosphere and ground. MODTRAN provides seven standard atmospheres for different latitudes and seasons of the year on the Earth. In addition a database of spectral albedos for different soil types is available to determine ground radiance.

Based on the observer – aircraft geometry MIRA creates an interpolation database to determine radiance and transmittance along rays (paths) through the atmosphere. Altogether four different types of paths occur: From observer to sky/ground, from aircraft to sky/ground, from observer to aircraft, and within the aircraft bounding volume. The interpolation variable for paths to sky/ground is the zenith angle. Along rays from observer to aircraft and within the aircraft bounding volume the interpolation variable is path-length. Instead of starting many successive MODTRAN runs, MIRA uses parallel MODTRAN runs for each of the four types of paths. Thus, in optimal conditions (enough memory and free CPUs/cores) the generation of the interpolation database requires the calculation time of about four MODTRAN runs. In fact, the creation of the atmospheric interpolation database is usually a matter of a few seconds only.

Realistic ground model

A short-coming of employing MODTRAN in the way just described, is that the ground is always modeled as a homogeneous surface. In reality, however, variations in ground radiance (“clutter”) may greatly influence the detectability of an airplane that is observed against the ground. Therefore, MIRA´s ground model was extended to permit use of digital elevation models (DEM) in connection with surface classifications. The latter provide information regarding the type of soil on the DEM surface. This information can be obtained from satellite data. For use in MIRA the classification data is turned into BRDF textures which are mapped onto the respective DEM. In this manner, MIRA is able to determine spatially resolved ground emissivity. Temperature distributions on the ground are also defined by use of textures. With this extension MIRA is able to model a flight over existing terrain and the realism of calculated images is greatly enhanced.

3. AERODYNAMIC ASSESSMENT

The MULDICON configuration is the result of a longer lasting effort in aerodynamic UCAV design. This research led to Lambda wing type

planforms with medium sweeps of the leading edge. MULDICON´s predecessor was the DLR-F17 which was based to large extends on the SACCON design developed by EADS-MAS (now ADS).

Fig. 2 shows the main geometrical details of the MULDICON planform. MULDICON´s leading edge sweep is 53°, the wingspan is 15.38 m and the airfoil is based on a NACA 64A001 design. From an aerodynamic point of view there is a great similarity to the SACCON configuration, for which many wind tunnel investigations and comparisons to TAU and other CFD models have been performed [10, 11, 12].

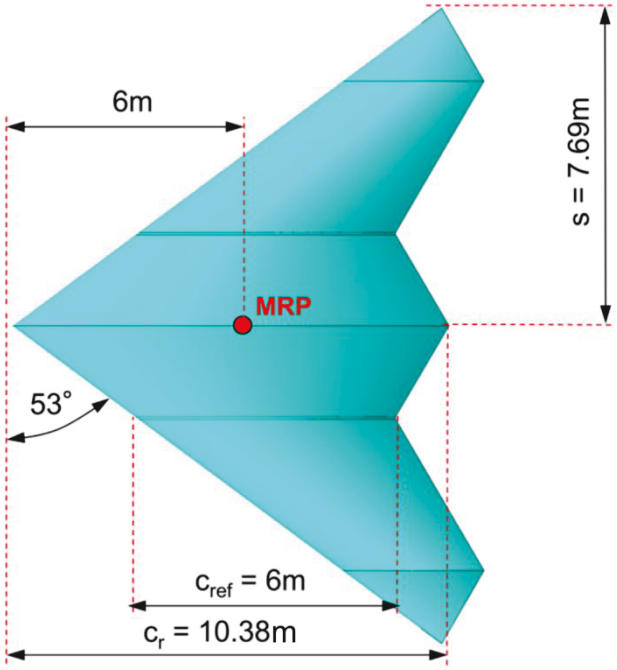

Fig. 2 Geometrical details of the MULDICON planfrom.

Grid generation

To keep the number of grid cells at a manageable level, unnecessary details such as gaps, hints and actuator parts are omitted from the CFD grid. However, parts relevant to the IR signature assessment are added. This regards an inlet tube and an exhaust duct. As it is planned to perform radar signature calculations with the same grid in the future, the local spatial resolution of the grid has been increased particularly at the wing leading and trailing edges, and at the transition body/wing-box. A highly resolved grid is also generated at the aft of the airplane. Here it is required to correctly describe the mixing of the exhaust jet with the external flow that separates from the aircraft body.

The commercial software *Centaur* [13] was employed to create the grid. Grid generation is based on a hybrid, structured and unstructured, approach in which different polygonal cell types are used. The resulting mesh which represents MULDICON consists of prismatic cells in pseudo structured layers at the walls. The rest of the calculation domain is filled with tetrahedral elements.

Prerequisite to the generation of the final grid was a study to determine meshing parameters which yield the required mesh resolution to resolve the main flow features within the exhaust duct. For this task the *grid adaptation technology* [14] was applied. The resulting grid consists of about 30 million points and 63 million cells (31 million tetrahedrons and 32 million prisms). There are 30 pseudo structured layers at the walls. This number of layers seems quite large. However, the turbulence model (Spalart-Allmaras) definitely needs them. They are also required to determine correct surface temperatures.

High spatial grid resolution is furthermore required to predict the jet characteristics and its mixing with ambient air close to the nozzle exit. Getting this right is decisive, as it determines the exhaust gas temperature which greatly affects the IR signature.

Flow simulation

As mentioned above DLR´s compressible, finite volume solver TAU was used to determine the aerodynamic properties of the flow in the exhaust duct as well as around and behind MULDICON. TAU is well validated by many experimental and numerical validation campaigns. The simulations performed were steady Reynolds Averaged Navier-Stokes (RANS) calculations. The following methods were used in the calculations:

- TAU´s “AUSDV” flux splitting scheme
- Backward Euler scheme as relaxation solver
- Green-Gauss scheme to reconstruct gradients
- Implicit residual averaging and 3-w multi-grid cycles to accelerate the calculation

Turbulence modeling in separating flows is still challenging. As it is known that the one-equation Spalart-Allmaras turbulence model yields a good wall shear stress representation

even for separated flows, it was employed in the calculations for this work.

Regarding the boundary conditions the following assumptions were made:

The far-field is modeled as an undisturbed flow on a sphere with a radius of 100 times the airplane length. Fuselage, wings, and internal surfaces are viscous no-slip walls. Furthermore, thermal adiabatic surfaces are assumed.

MULDICON is equipped with a variable cycle engine. However, the engine is not explicitly modeled. Rather, the engine is represented by two aerodynamic interface planes. One is at the end of the inlet tube, close to the compressor. The other is shortly after the low pressure turbine. The core jet and the bypass air flow through this boundary into the exhaust duct.

The interface plane at the inlet has a “pressure exit outflow” boundary condition assigned with a static pressure of 280 hPa. The entry to the exhaust duct is modeled as “total pressure inflow” boundary. In the core region the total pressure is 4990 hPa and the temperature is 640 K. The values in the bypass section are: Total pressure 620 hPa and temperature 520 K.

The considered flight and ambient conditions are an altitude of 11 km, a pressure of 227 hPa, a temperature of 217 K and a speed of Mach 0.8 (236 m/s). This leads to a Reynolds number of about 36 million. The aircraft angle of attack was set to 3°.

4. EXHAUST DUCT DESIGN

In comparison to the DLR-F17 a major change was introduced in the MULDICON configuration which regards the exhaust duct and thus affects the IR emission of the exhaust gas. The DLR-F17 has one common duct for bypass and core. This causes a certain degree of mixing before the gases are released to the atmosphere, where further mixing with ambient air takes place. The MULDICON exhaust duct is designed to enforce a much higher degree of mixing already within the duct. The objective is to achieve a much lower exhaust gas temperature and consequently a greatly reduced IR emission at the exhaust duct exit.

As depicted in Fig. 3 the MULDICON intake tube and the exhaust duct are curved to decrease the range of aspect angles from which the compressor or the low pressure turbine are directly visible. This is very similar to the DLR-F17.

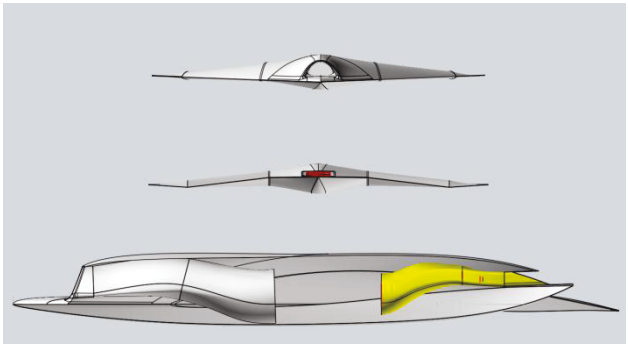

Fig. 3 **Views on MULDICON. Top: Front aspect with the central inlet. Middle: Rear aspect with the exhaust duct (red). Bottom: Longitudinal cut which uncovers the curved intake tube and the bent exhaust duct (yellow).**

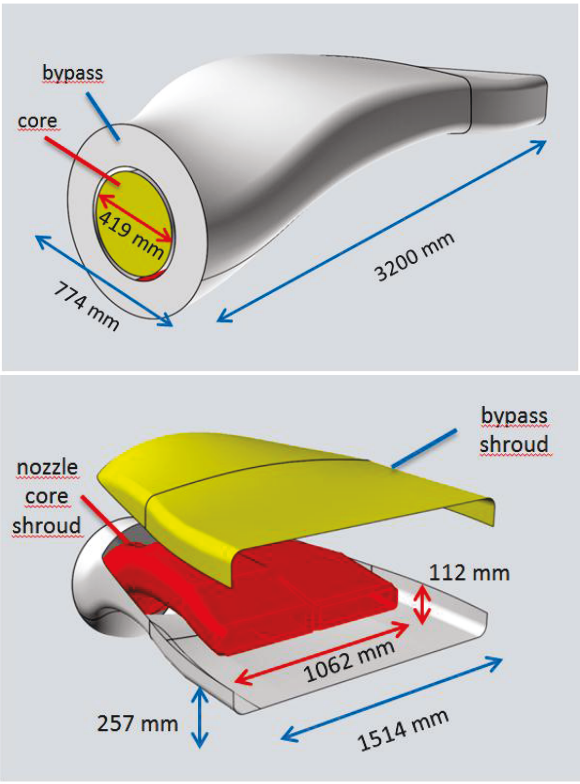

Fig. 4 **The internal curved exhaust duct. Top: Duct entry with the core and bypass sections marked. Bottom: Shroud of the core jet (red). This shroud separates the combustion gases and ends before the bypass shroud to enhance mixing inside the exhaust duct.**

The new part introduced in MULDICON is an additional core shroud which splits the core jet as depicted in Fig. 4. This element keeps bypass air and core jet separated for a certain length and additionally splits the core jet.

The advantage with this design is improved mixing of core and bypass after the core shroud but still inside the exhaust duct. In this way the temperatures and thus the IR emission of the exhaust gases that become visible after ejection to the atmosphere are lowered very effectively.

The effect is demonstrated in Fig. 5 (DLR-F17) and Fig. 6 (MULDICON) which show the temperature distributions as predicted by TAU for the same flight conditions.

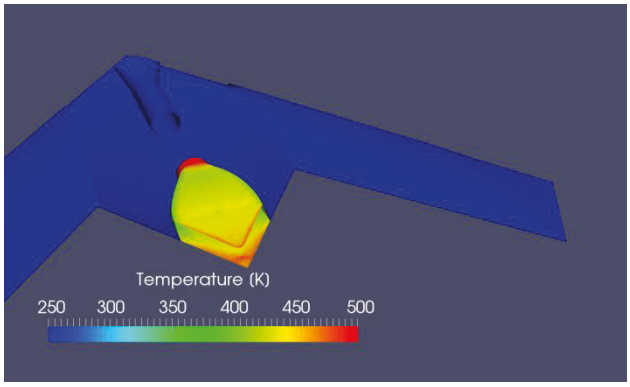

Fig. 5 Temperature distribution on the exhaust duct of DLR-F17. The central upper part of the airframe is removed to show the duct.

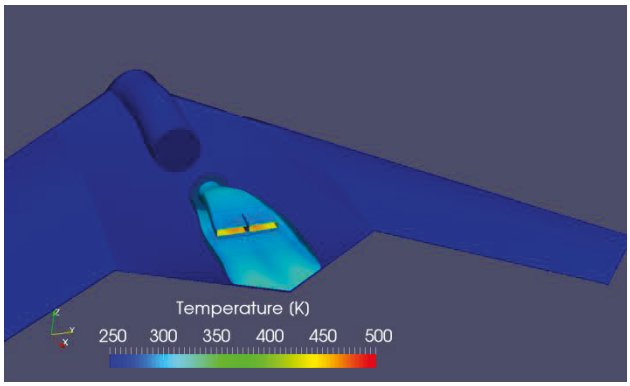

Fig. 6 Temperature distribution on the exhaust duct of MULDICON. The central upper part of the airframe is removed to show the duct.

It must be emphasized that Fig. 5 and Fig. 6 regard the same *flight* conditions. In fact, by comparing the technical data of the propulsion system of both designs, one might expect a different result:

The engine of the DLR-F17 has a maximum thrust of 35 kN and a bypass ratio of 2. MULDICON achieves 60 kN maximum thrust. The latter configuration has a variable cycle engine (VCE) installed with a maximum bypass ratio of 1.3. Thus, one expects that MULDICON´s exhaust gas temperature is higher. In fact, the MULDICON exhaust gas at the duct entry with a temperature of 616 K is slightly warmer (22 K) than the DLR-F17´s exhaust gas with 594 K.

However, from Fig. 5 and Fig. 6 it is evident that the MULDICON exhaust duct lowers the temperature at the end of the duct considerably to about 320 K, i.e. the temperature decreases by 296 K. With about 450 K the DLR-F17 is much hotter at this station. The DLR-F17 duct reduces the temperature by only 144 K. The temperature difference of the two configurations at the duct exit is 130 K. This demonstrates the improved efficiency of the new exhaust duct design.

5. IR SIGNATURE COMPARISON

In this section the IR signature of MULDICON and its predecessor, the DLR-F17, are compared. The flight conditions are the same that were used for the flow field calculation presented above, i.e. flight altitude 11 km and speed Mach 0.8. A worst case scenario is assumed: The sky is clear and the ground is homogeneous. For the latter the albedo is set to 0.4. The considered wavelength range is 3.33 – 5.0 µm. This is typical for aircraft detection, as it includes the very temperature sensitive CO_2 emission band centered at 4.3 µm. Observer and aircraft are 5 km apart.

The IR signatures are determined by MIRA for three aspects. Two of them regard the exhaust duct with an off-tail angle of 45° between the aircraft roll axis and the sensor line of sight. The view is directed onto the aircraft from the top, with an elevation of 35°, and from the bottom (elevation –35°). The predicted IR signatures of both configurations for these aspects are shown in Fig. 7 to Fig. 11. Note that these figures as well as Fig. 11and Fig. 12 display radiance temperatures, in contrast to Fig. 5 and Fig. 6, which show physical temperatures.

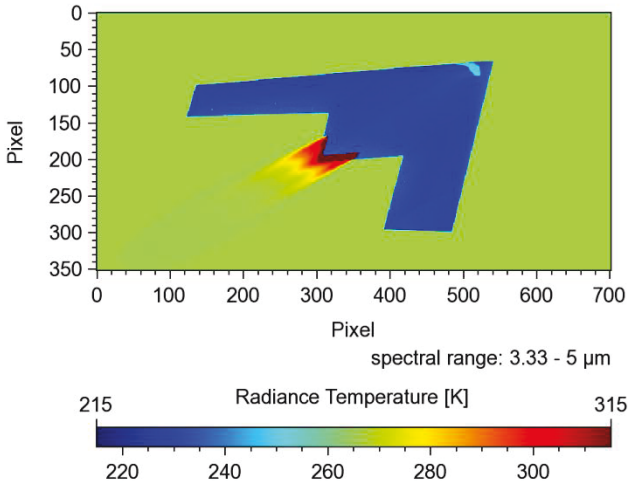

Fig. 7 **IR signature of DLR-F17S. Aspect angles: Off-tail = 45°, Elevation = 35°.**

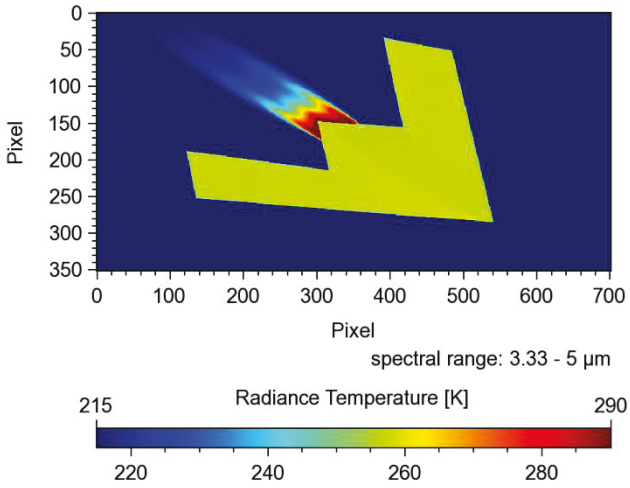

Fig. 8 **IR signature of DLR-F17. Aspect angles: Off-tail = 45°, Elevation = -35°.**

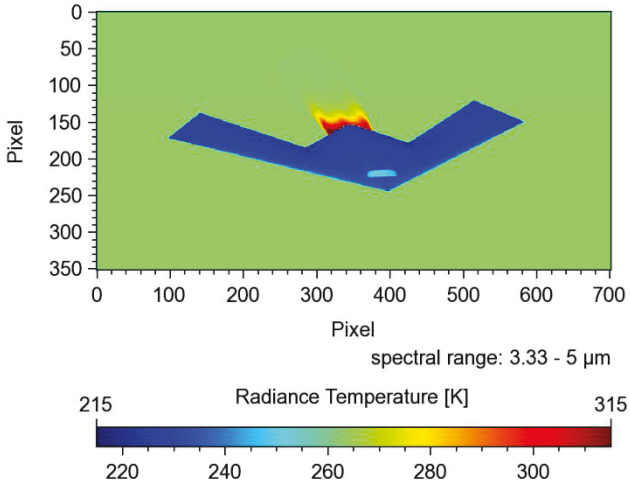

Fig. 9 **IR signature of DLR-F17. Aspect angles: Off-tail = 170°, Elevation = 15°.**

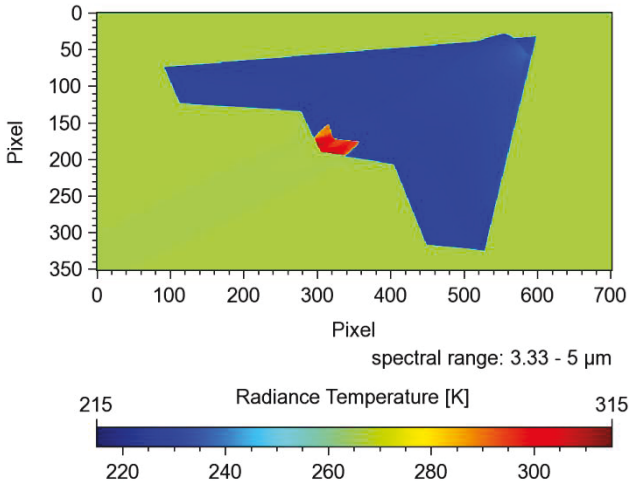

Fig. 10 **IR signature of MULDICON. Aspect angles: Off-tail = 45°, Elevation = 35°.**

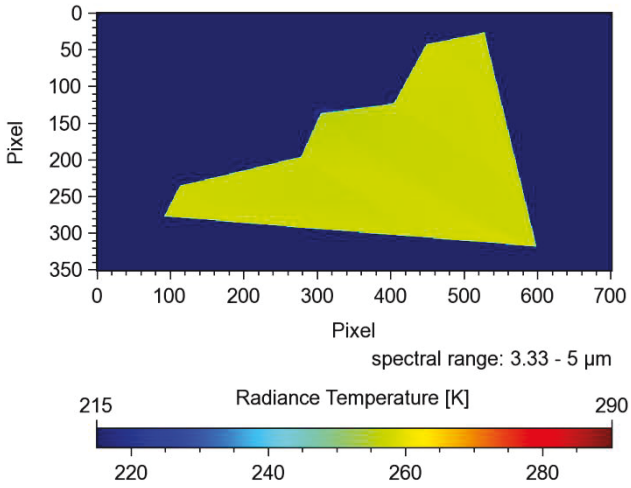

Fig. 11 **IR signature of MULDICON. Aspect angles: Off-tail = 45°, Elevation = -35°.**

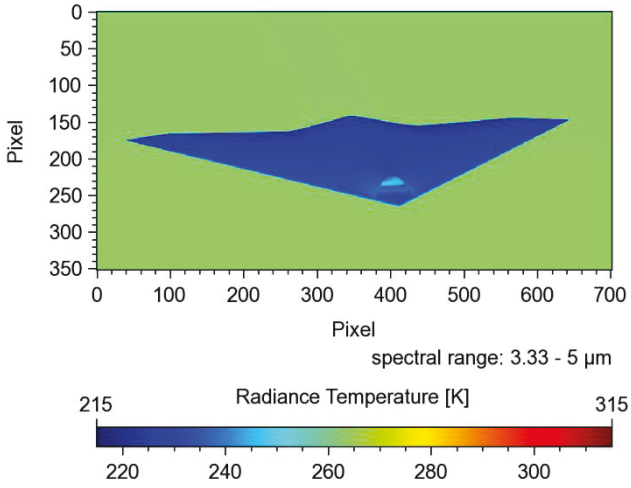

Fig. 12 **IR signature of MULDICON. Aspect angles: Off-tail = 170°, Elevation = 15°.**

Fig. 9 and Fig. 12 provide the results for the third aspect, the view on the front with an off-tail angle of 170° and an elevation of 15°. Fig. 9 shows that even for this small elevation angle the DLR-F17 exhaust gases are the major source of radiance. It can also be noticed that the front shape of MULDICON´s inlet hides a large part of the inlet IR radiation. The DLR-F17 is lacking such feature.

On the other hand, by comparison of Fig. 7 and Fig. 10, which show views on the exhaust ducts of both configurations from above, it becomes clear that a similar hiding effect would be desirable for the MULDICON exhaust gas exit which in the current design forms a hot spot with relatively large area. From the IR signature point of view an extension of the upper side of the MULDICON central part would be advisable to achieve such shielding.

However, regarding the IR radiation emitted by the MULDICON exhaust gas, its emission is not discernible from the background in any of the signature images (Fig. 10, Fig. 11, and Fig. 12). In contrast, the gases released from the DLR-F17 generate a certainly appreciable amount of radiation.

6. MULDICON OVER REALISTIC GROUND

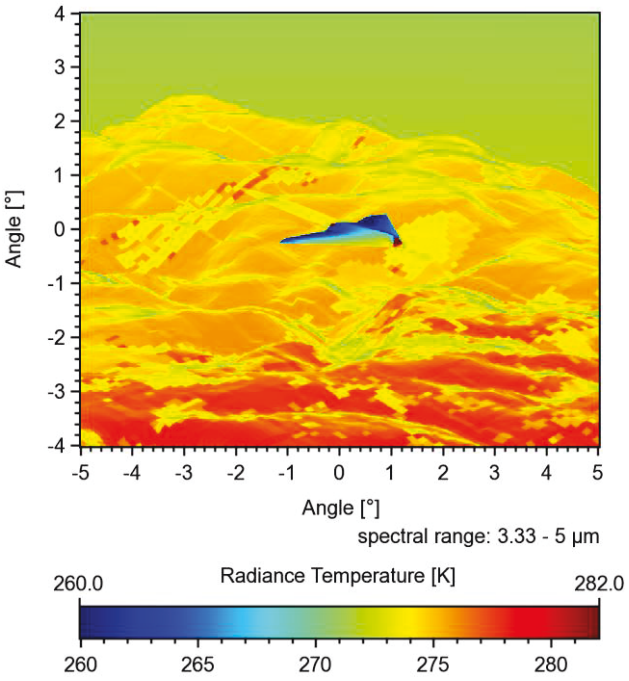

Fig. 13 IR signature of MULDICON flying in front of mount Brocken in the Harz area of Germany.

Fig. 13 shows an example of MIRA´s capability to model realistic ground. The landscape chosen for this simulation is the Harz area in Germany. DEM and classification cover an area of 135 km x 110 km and were provided by DLR´s German Remote Sensing Data Center (DFD). The excerpt shown in Fig. 13 shows MULDICON flying at an altitude of 4,980 m and a velocity of Mach 0.8 in front of mount Brocken. The camera field of view is 10° x 8.3° and the aspect angles are off-tail 135° and elevation 15°. In the signature image the exhaust gas behind the aircraft is visible as a faint jet. The reason for this is the small distance between aircraft and camera of 300 m. In Fig. 7 to Fig. 12 this distance is 5,000 m. Nevertheless, the exhaust gas emission is not very different from that of other areas in the structured background. More important is the low emission from the wings which is caused by the low ambient temperatures at the flight altitude of nearly 5 km. The resulting negative contrast against the background would obviously lead to detection and tracking of the vehicle.

7. SUMMARY

This contribution provided details regarding the IR signature assessment of a generic UCAV configuration, called MULDICON, which was used to demonstrate a multi-disciplinary design approach within the frame of the DLR project Mephisto. Part of the work carried out in this project was the extension of DLR´s IR signature model MIRA. The added capabilities comprise a multi-reflection model and the modeling of real terrain by use of geo-physical satellite data. This latter feature greatly improves the realism of the simulations by provision of a structured background.

A crucial input to IR signature simulations of air vehicles are results from CFD calculations. These provide pressure, temperature, and species concentrations in the exhaust jet as well as aircraft surface temperatures. Within Mephisto DLR´s flow solver TAU was employed for this task.

Finally, MIRA results for a worst case scenario show the progress achieved regarding the IR signature caused by the propulsion system. By comparison to an earlier configuration (DLR-F17) it is demonstrated that despite a much higher thrust and smaller bypass ratio the IR

signature of the exhaust gases is greatly reduced.

However, the airplane as a whole is in most situations clearly detectable. The reasons are effects caused by the vehicle surfaces. In observations against the ground, the surfaces are in general colder than the ground, leading to lower IR emissions and thus to a negative contrast. If the aircraft is viewed against the clear sky, radiance emitted by the warm ground is reflected at the aircraft which causes a positive contrast.

Therefore, the improvement of the exhaust duct was only a first step. More effort is needed to create a well camouflaged aircraft.

[1] Lindermeir, E. (2011). “Recent Advances in Aircraft IR Signature Modeling at DLR”. 7th International IR Target and Background Modeling & Simulation Workshop, 27-30 June 2011, Toulouse, France

[2] Lindermeir, E. and M. Rütten (2014). “MIRA - An IR Signature Model for Unmanned Aerial Vehicles (UAV)”. Optro 2014 - 6th International Symposium on Optronics in Defence and Security , 28-30 Jan. 2014, Paris, France

[3] Gerhold, T., Evans, J. (1999). “Efficient Computation of 3D-Flows for Complex Configurations with the DLR Tau-Code Using Automatic Adaptation”, Notes on Numerical Fluid Mechanics, vol. 72, Vieweg

[4] Veach, E. (1998). Robust Monte Carlo methods for light transport simulation, PhD thesis, *Stanford University, Stanford, CA, USA*.

[5] Rothman, L.S., Gordon, I.E., Barber, R.J., Dothe, H., Gamache, R.R., Goldman, A., Perevalov, V.I, Tashkun, S.A., Tennyson, J. (2010). HITEMP, the high-temperature molecular spectroscopic database. *J. Quant. Spectrosc. Radiat. Transfer*, 111, 15, S. 2139-2150.

[6] Ludwig, C.B., Malkmus, W., Reardon, J.E., Thomson J.A.L. (1973). Handbook of Infrared Radiation from Combustion Gases. *NASA report SP-3080, Scientific and Technical Information Office, Washington D.C.*.

[7] Lindermeir, E., Beier, K. (2012). HITEMP derived spectral database for the prediction of jet engine exhaust infrared emission using a statistical band model. *J. Quant. Spectrosc. Radiat. Transfer*, 113, 1575–1593.

[8] Berk, A., P.K. Acharya, L.S. Bernstein, G.P. Anderson, J.H. Chetwynd, Jr., M.L. Hoke (2000). Reformulation of the MODTRAN band model for finer spectral resolution, *Proc. SPIE* Vol. 4049, Algorithms for Multispectral, Hyperspectral, and Ultraspectral Imagery VI.

[9] Berk A., G.P. Anderson, P.K. Acharya, E.P. Shettle (2011). MODTRAN 5.2.1 User’s Manual. *Spectral Sciences, Inc., Fourth Ave., Burlington, MA 01803-3304*.

[10] Schütte, A. (2010). “Numerical and Experimental Analyses of the Vortical Flow Around the SACCON Configuration”, 28th AIAA Applied Aerodynamics Conference, AIAA-2010-4690

[11] Vallespin, D., Da Ronch, A. and Badcock, K.J. (2010). “Validation of Vortical Flow Predictions for a UCAV Wind Tunnel Model”, 28th AIAA Applied Aerodynamics Conference, AIAA-2010-4690

[12] Cummings, R. (2010) “SACCON Static and Dynamic Motion Flow Physics Simulations Using COBALT”, 28th AIAA Applied Aerodynamics Conference, AIAA-2010-4691

[13] www.centaursoft.com

[14] Alrutz, T., Rütten, M. (2005). Investigation of Vortex Breakdown over a Pitching Delta Wing applying the DLR TAU-Code with Full, Automatic Grid Adaptation. *AIAA-2005-5162, Toronto, Canada*.